Probe axion-like particles at the electron-ion collider

In collaboration with Reuven Balkin, Or Hen, Wenliang Li, Teng Ma, Christoph Paus, Yotam Soreq, Michael Williams

Hongkai Liu

TECHNION
Israel Institute of Technology

The 6th EicC CDR workshop, Huizhou
December 19-22, 2023

The Electron ion collider (EIC)

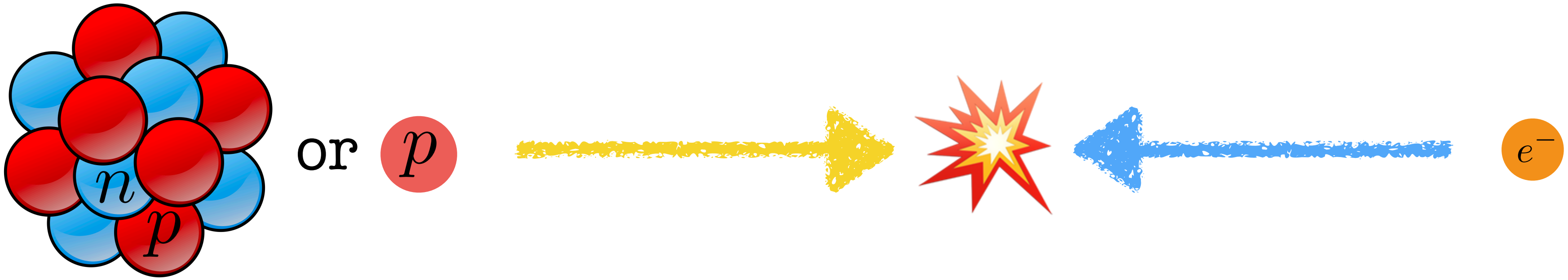

High energy:

$$E_e = 18\ \text{GeV}$$

$$E_p = 100\ (275)\ \text{GeV. For lead, } E_{\text{lead}} = 20\ \text{TeV}$$

High luminosity:

$$L_{\text{peak}} = 10^{33} - 10^{34}\text{cm}^{-2}\text{s}^{-1}$$

- Most of its key physics topics are achievable with 10/fb, corresponding to 30 weeks of running assuming 60% operation efficiency and $10^{33}\text{cm}^{-2}\text{s}^{-1}$ peak luminosities
- The study of the spatial distributions of quarks and gluons in the proton requires 100/fb.

The Electron ion collider (EIC)

- The different detector systems observe different particle distributions.

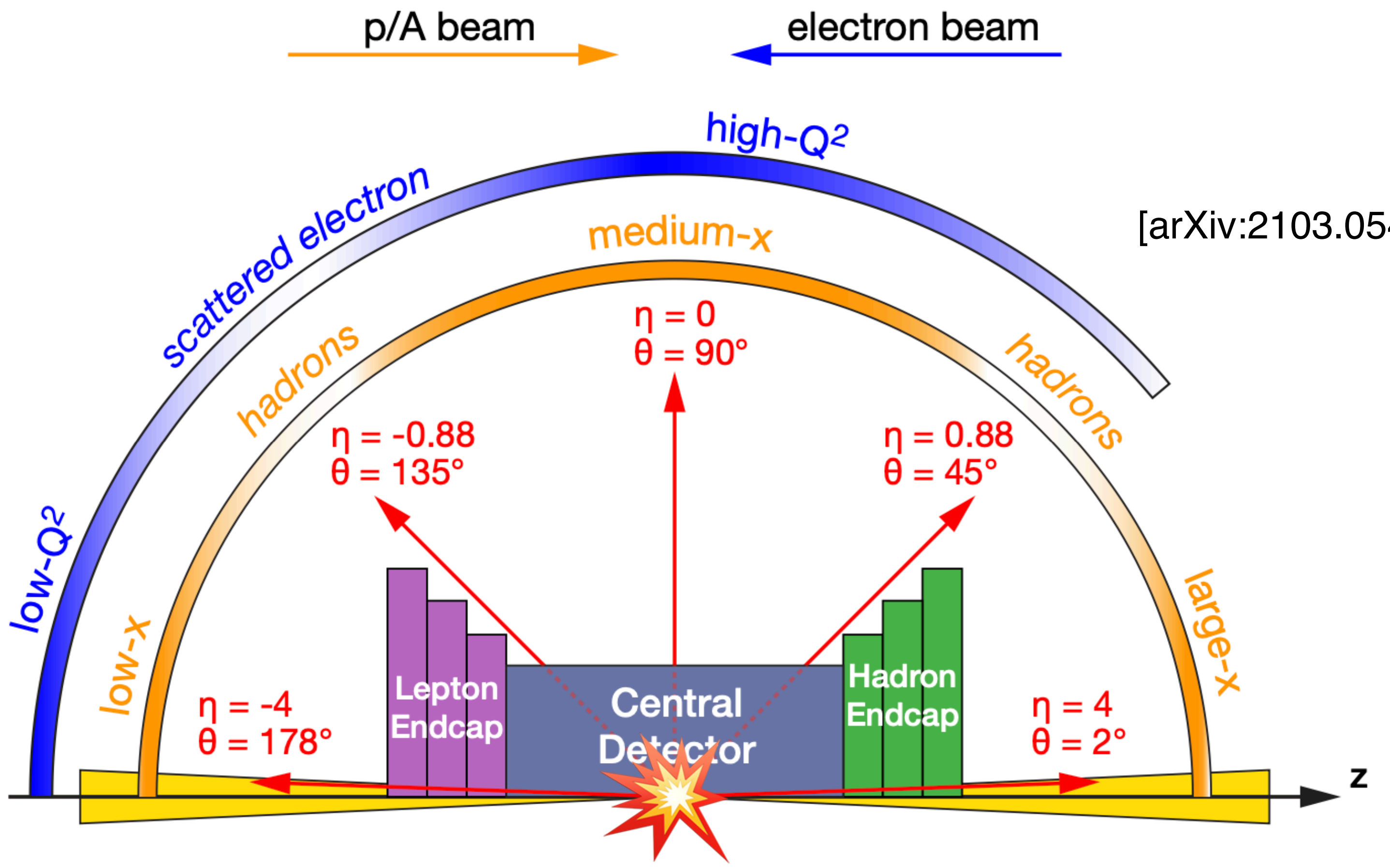

[arXiv:2103.05419]

The Electron ion collider (EIC)

- The different detector systems observe different particle distributions.

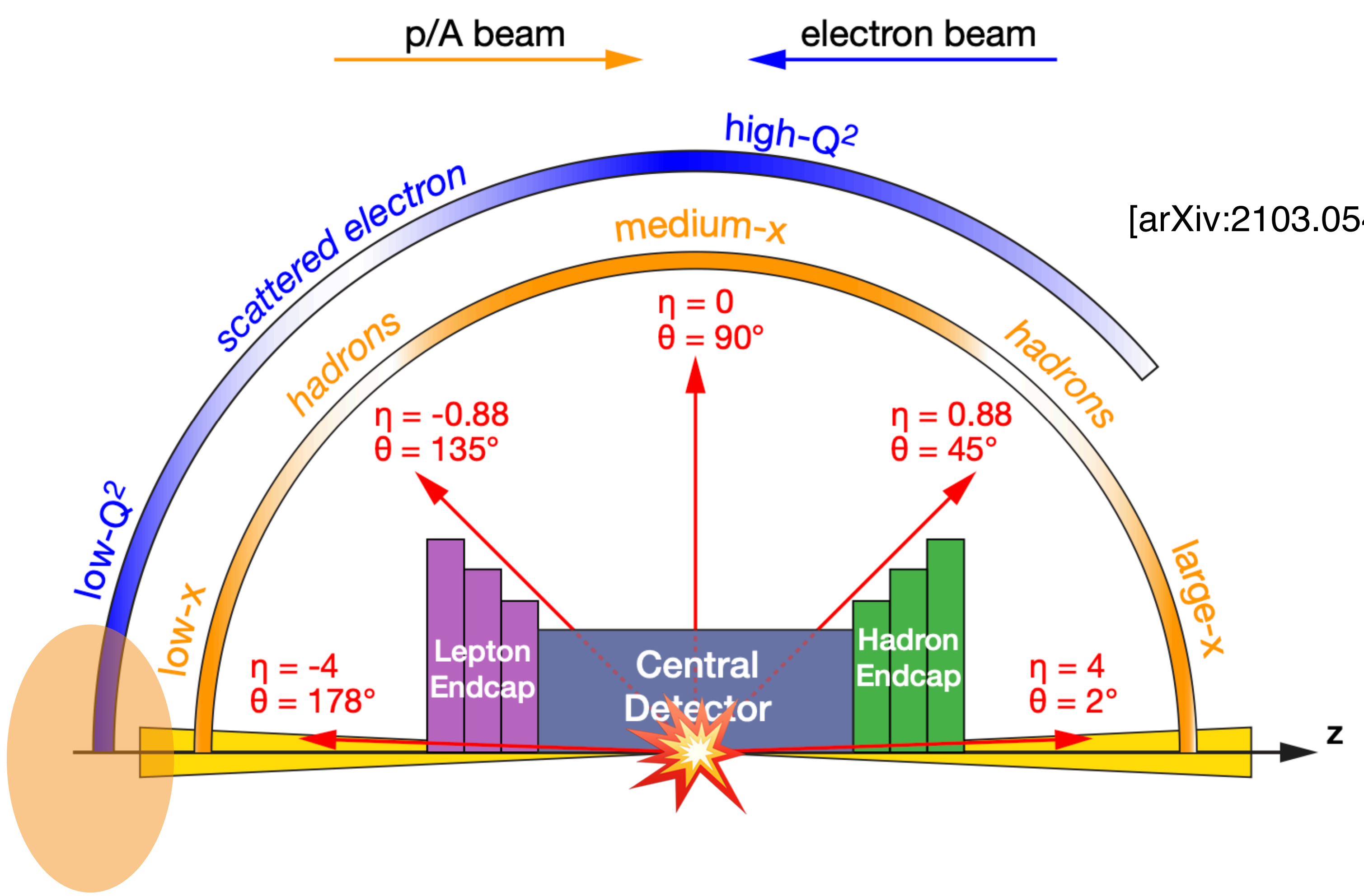

[arXiv:2103.05419]

Far-backward detector:
Measure scattered electrons with very low Q^2 and luminosity

Tagging recoiled electrons

[arXiv:2103.05419]

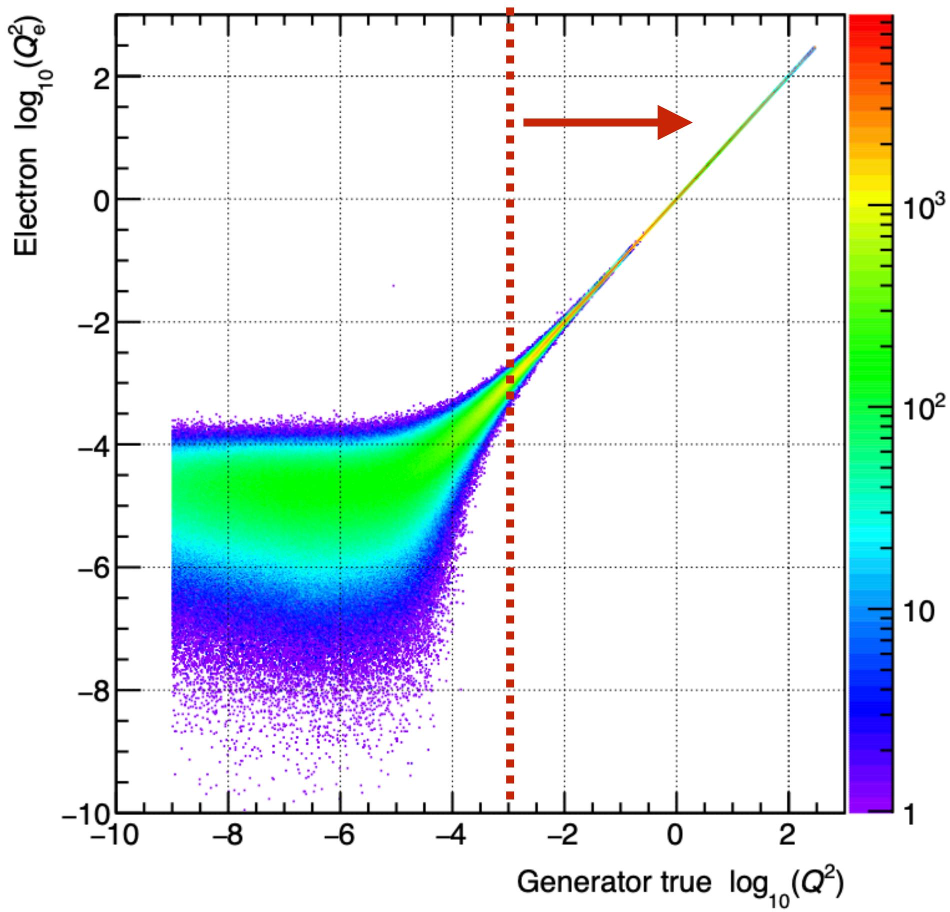

Figure 11.121: Comparison of generated and reconstructed electron Q_e^2 with smearing for beam angular divergence.

- Recoiled electrons with very low-Q^2 ($10^{-9}\ \mathrm{GeV}^2$) can be tagged.
- But only when $Q^2 > 10^{-3}\ \mathrm{GeV}^2$ we can have reasonable good resolution.

The Electron ion collider (EIC)

- The different detector systems observe different particle distributions.

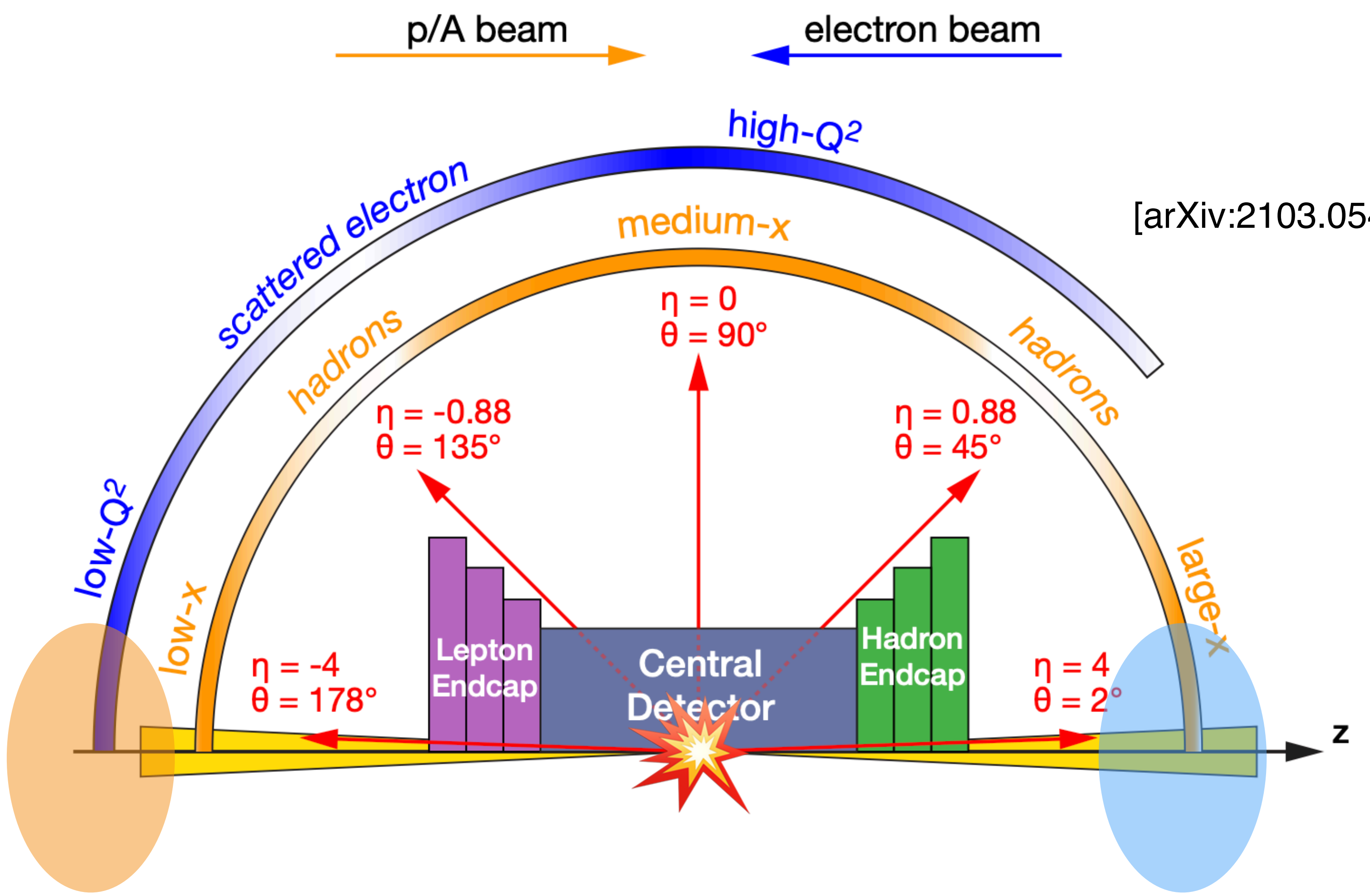

Far-backward detector: Measure scattered electrons with very low Q^2 and luminosity

Ideal for studying coherent scattering

Far-forward detector: Can select the coherent collision vetoing spectator neutrons from nuclear breakup

Motivation

$$\mathcal{L}_{\text{BSM}} = \mathcal{L}_{\text{SM}} + \mathcal{L}_{\nu\,\text{mass}} + \mathcal{L}_{\text{DM}} + \mathcal{L}_{\text{BA}} + \mathcal{L}_{\text{strong CP}} + \cdots$$

Motivation

- QCD axion is a solution to the strong CP problem.

$$\mathcal{L}_a = \frac{1}{2}(\partial_\mu a)^2 - \frac{1}{2} m_a a^2 + \frac{a}{f_a}\frac{g_s^2}{32\pi^2} G\tilde{G}$$

- In the simplest model, the relation between the axion mass and coupling are in a narrow band. However, in less minimum UV models, the mass-coupling relations can be shifted.

- To be UV independent, we adopt EFT description and treat the coupling and mass as two independent parameters $\longrightarrow$ axion-like particles (ALPs).

- Generally, ALPs are allowed to couple to both gauge bosons and fermions. Here, we only focus on investigating the ALP-photon coupling at the electron-ion collider (EIC).

$$\mathcal{L}_a = \frac{1}{2}(\partial_\mu a)^2 - \frac{1}{2} m_a a^2 + \frac{a}{4\Lambda} F\tilde{F}$$

Current bounds

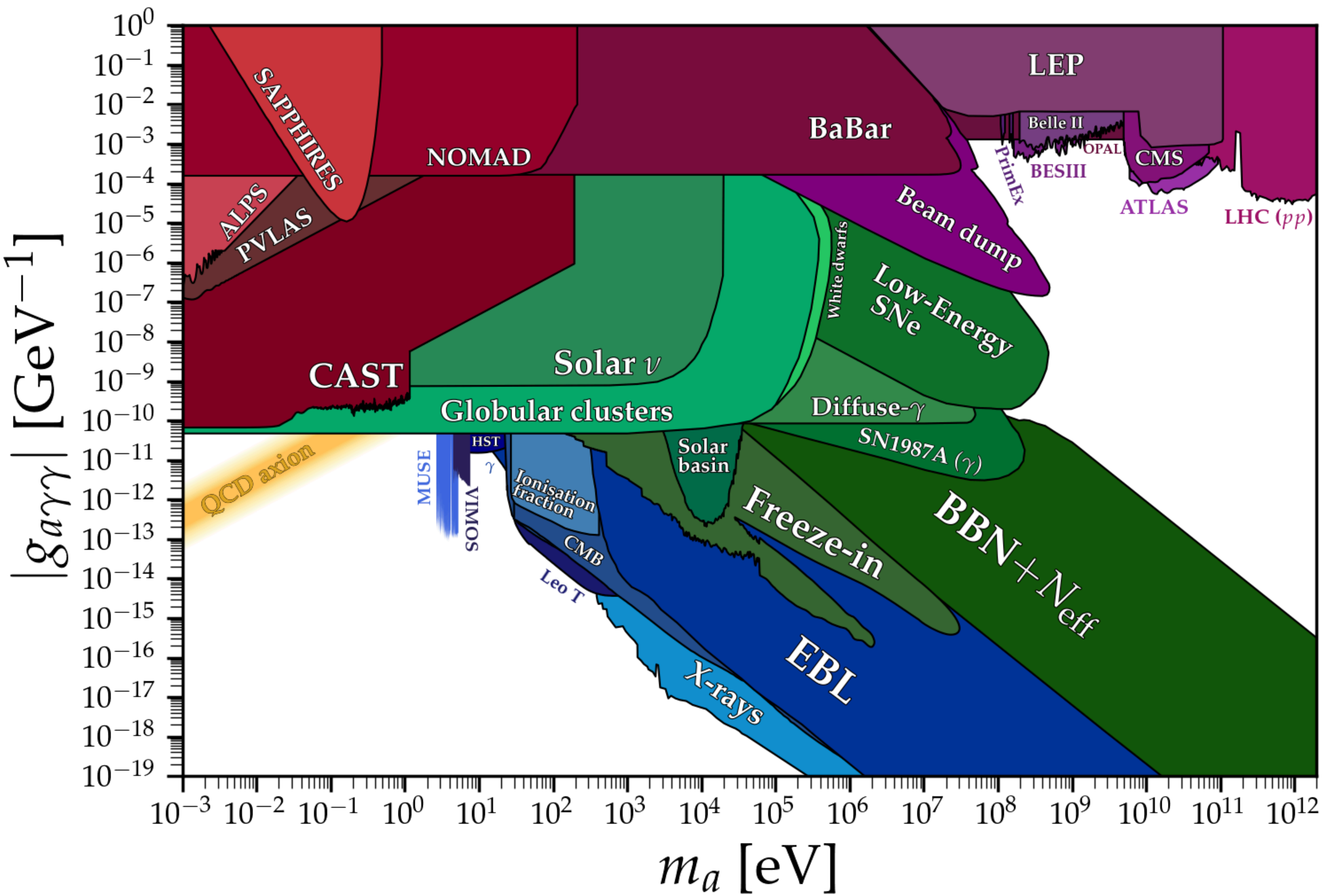

[https://github.com/cajohare/AxionLimits/blob/master/AxionPhoton_ColliderBounds.ipynb]

Current bounds

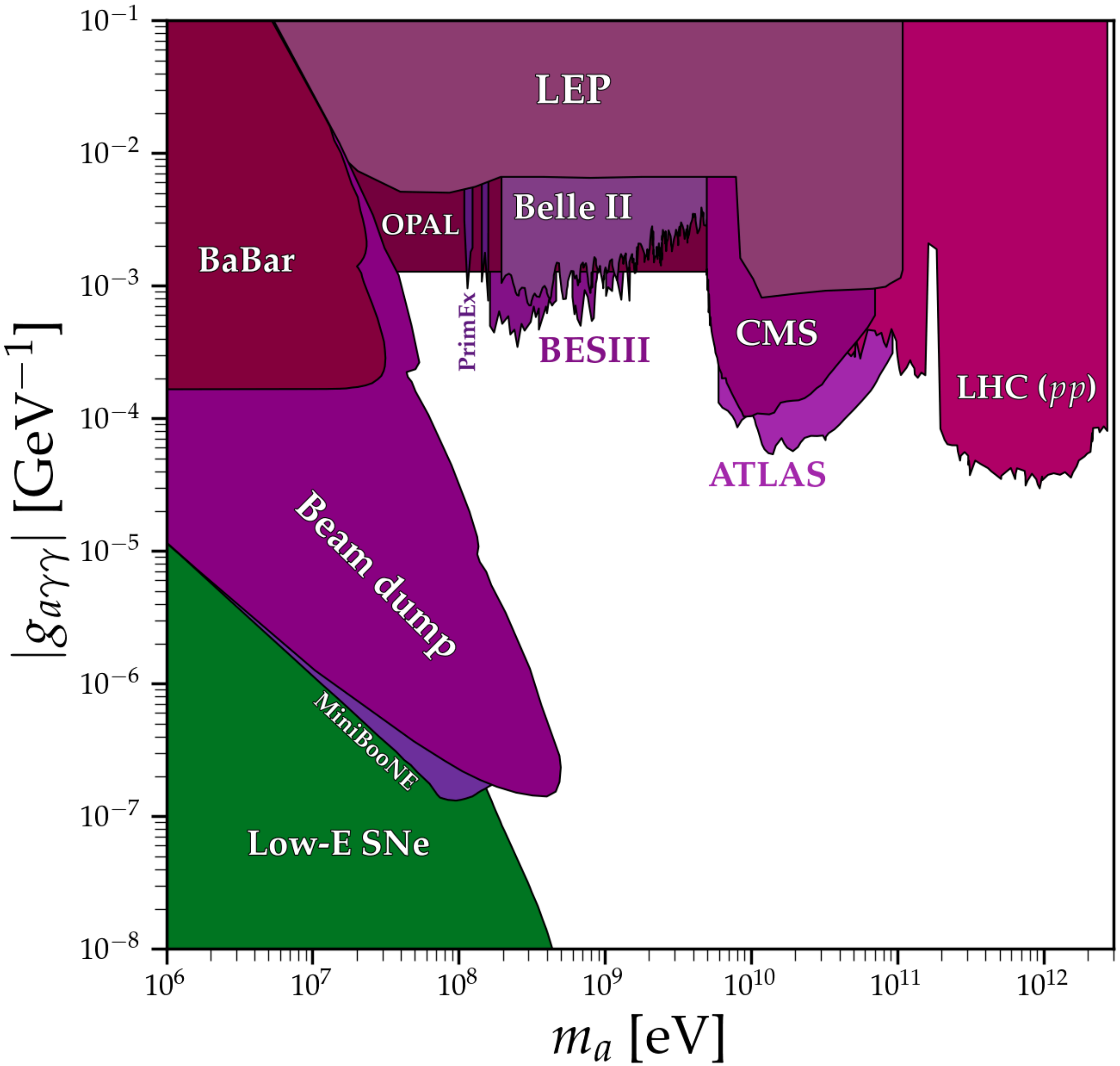

[https://github.com/cajohare/AxionLimits/blob/master/AxionPhoton_ColliderBounds.ipynb]

ALP coherent production at the EIC

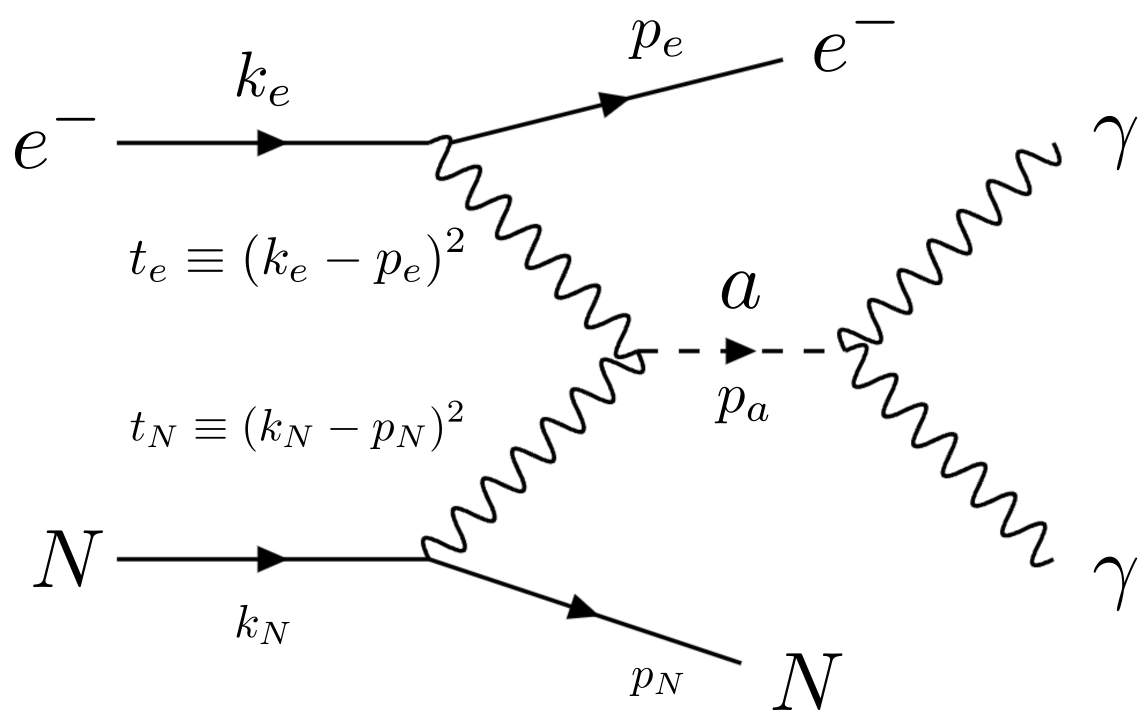

- Weakly coupled but with an enhancement of Z^2 in the ALP coherent production.

- The amplitude squared:

$$|\mathcal{M}_{2\to 3}|^2 \propto (Z^2 e^4)/(t_e^2 t_N^2 \Lambda^2)$$

- As the recoiled electron can be measured very precisely, the recoiled ion can be reconstructed:

$$p_N^2 = (k_e + k_N - p_a - p_e)^2 = m_N^2$$

Kinematics

$$(-t_N)_{\rm min} \approx 1.8 \times 10^{-8}\ {\rm GeV}^2 \left(\frac{m_a}{1.0\ {\rm GeV}}\right)^4 \left(\frac{m_N}{193\ {\rm GeV}}\right)^2 \left(\frac{\sqrt{s}}{1.2\ {\rm TeV}}\right)^{-4}$$

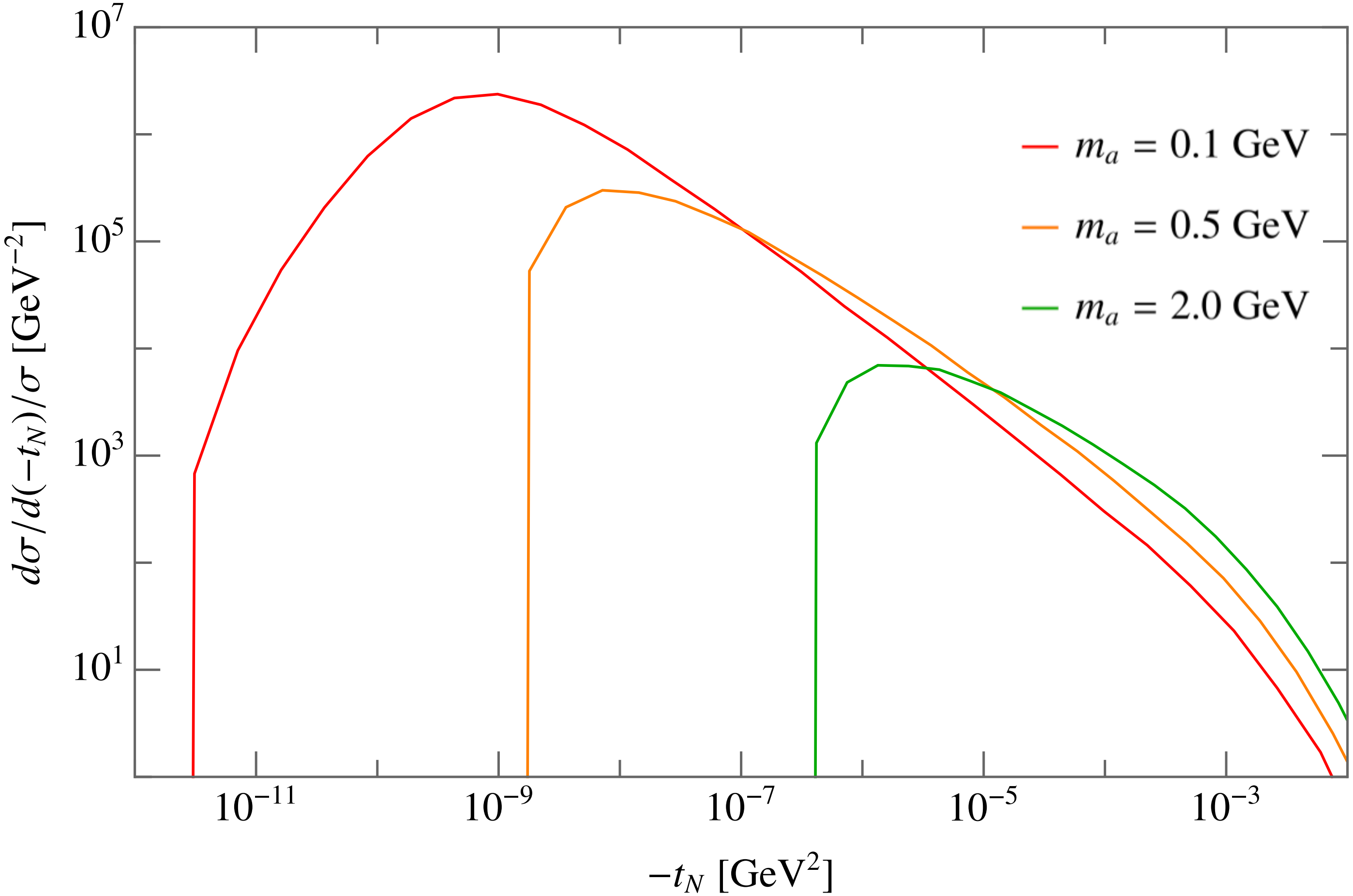

$$(-t_N)_{\rm min} \sim 0.164 A^{-2/3}\ {\rm GeV}^2 \longrightarrow [m_a]_{\rm max} \sim 20\ {\rm GeV} \left(\frac{E_e}{18\ {\rm GeV}}\right)^{1/2} \left(\frac{E_N/A}{100\ {\rm GeV}}\right)^{1/2} \left(\frac{A}{207}\right)^{-1/6}$$

[Above 20 GeV, inelastic scattering is dominant, Y. Liu, B. Yan, 2112.02477]

Kinematics

$$(-t_e)_{\min} \approx 1.9 \times 10^{-14}\ \mathrm{GeV}^2 \left(\frac{m_a}{1.0\ \mathrm{GeV}}\right)^2 \left(\frac{m_N}{193\ \mathrm{GeV}}\right)^2 \left(\frac{m_e}{0.51\ \mathrm{MeV}}\right)^2 \left(\frac{\sqrt{s}}{1.2\ \mathrm{TeV}}\right)^{-4}$$

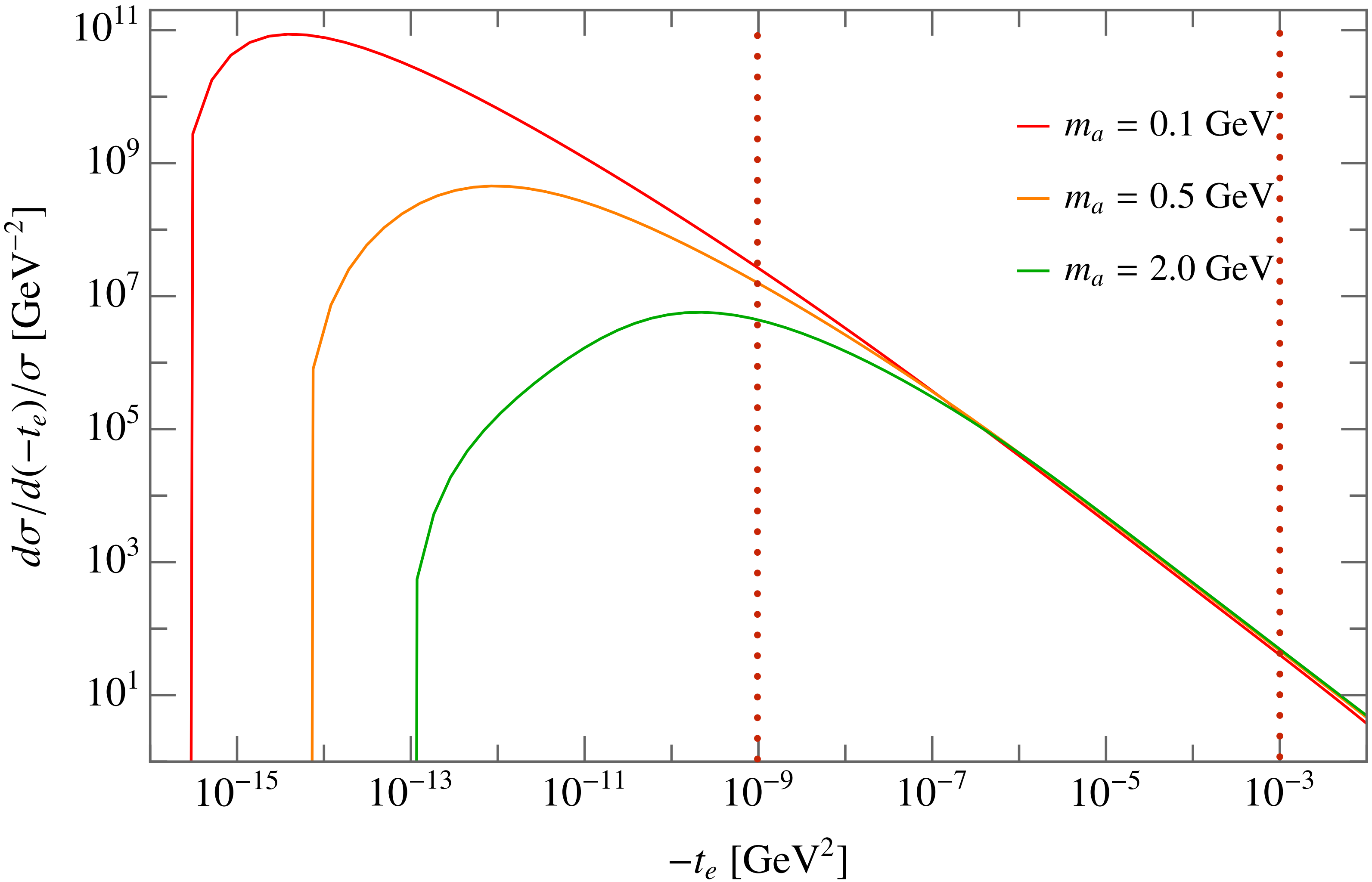

- The EIC can tag $-t_e > 10^{-9}\ \mathrm{GeV}^2$
- To obtain reasonable accuracy, we require $-t_e > 10^{-3}\ \mathrm{GeV}^2$

Efficiencies on te cut

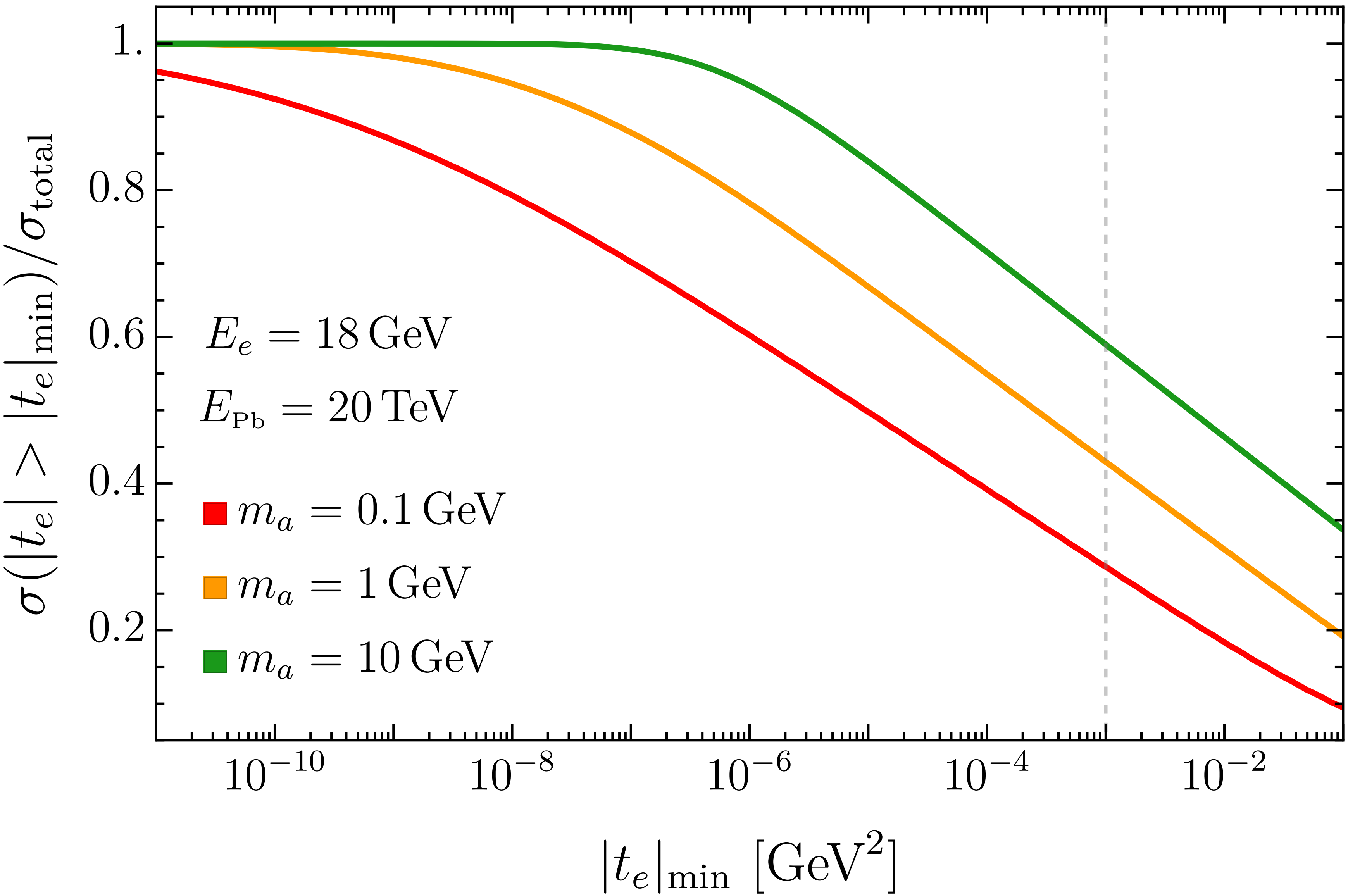

Kinematics

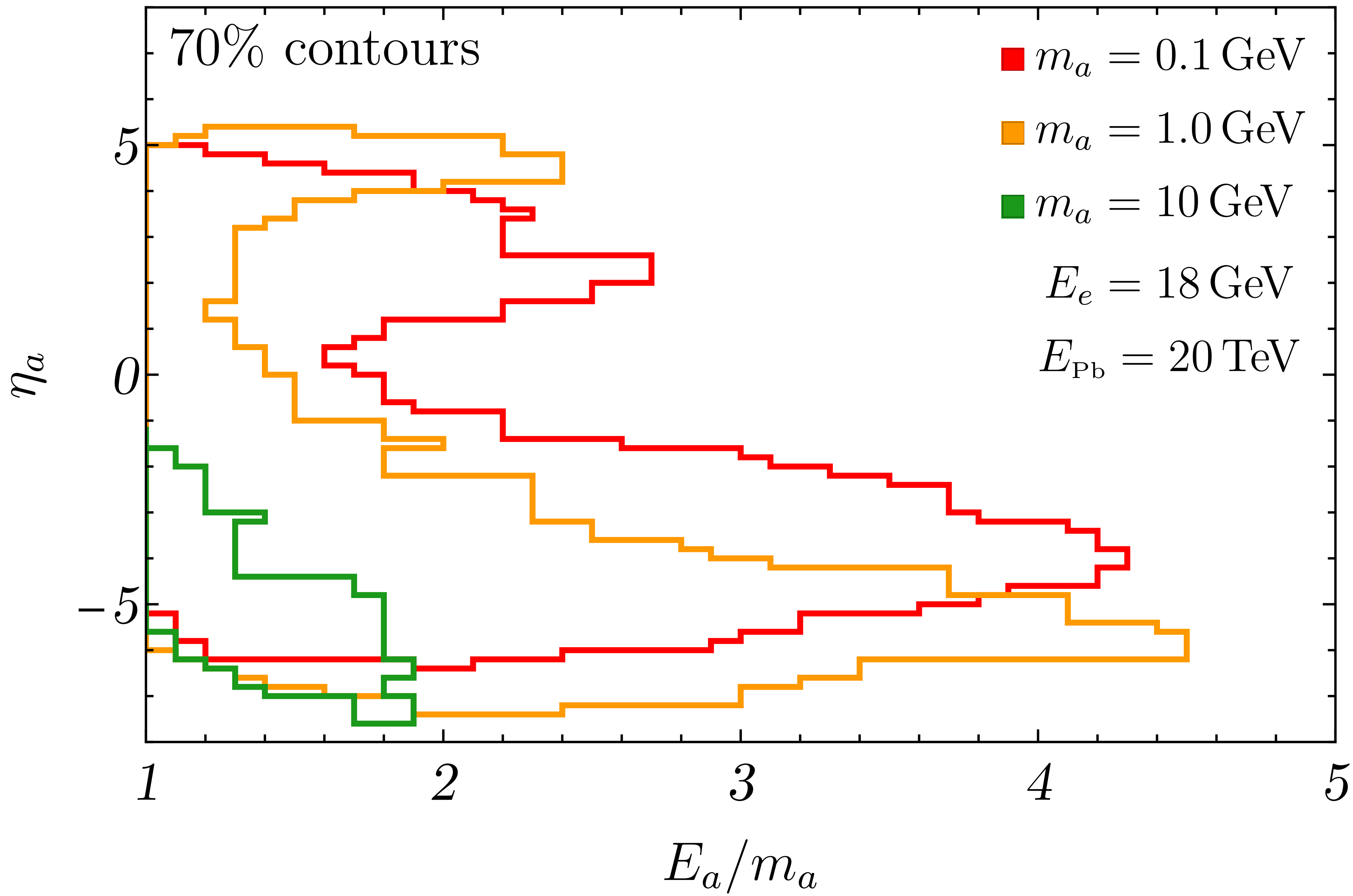

70% contours
$m_a = 0.1$ GeV
$m_a = 1.0$ GeV
$m_a = 10$ GeV
$E_e = 18$ GeV
$E_{\rm Pb} = 20$ TeV
η_a
5
0
−5
1
2
3
4
5
E_a/m_a

Merge efficiencies

[arXiv:2207.09437]

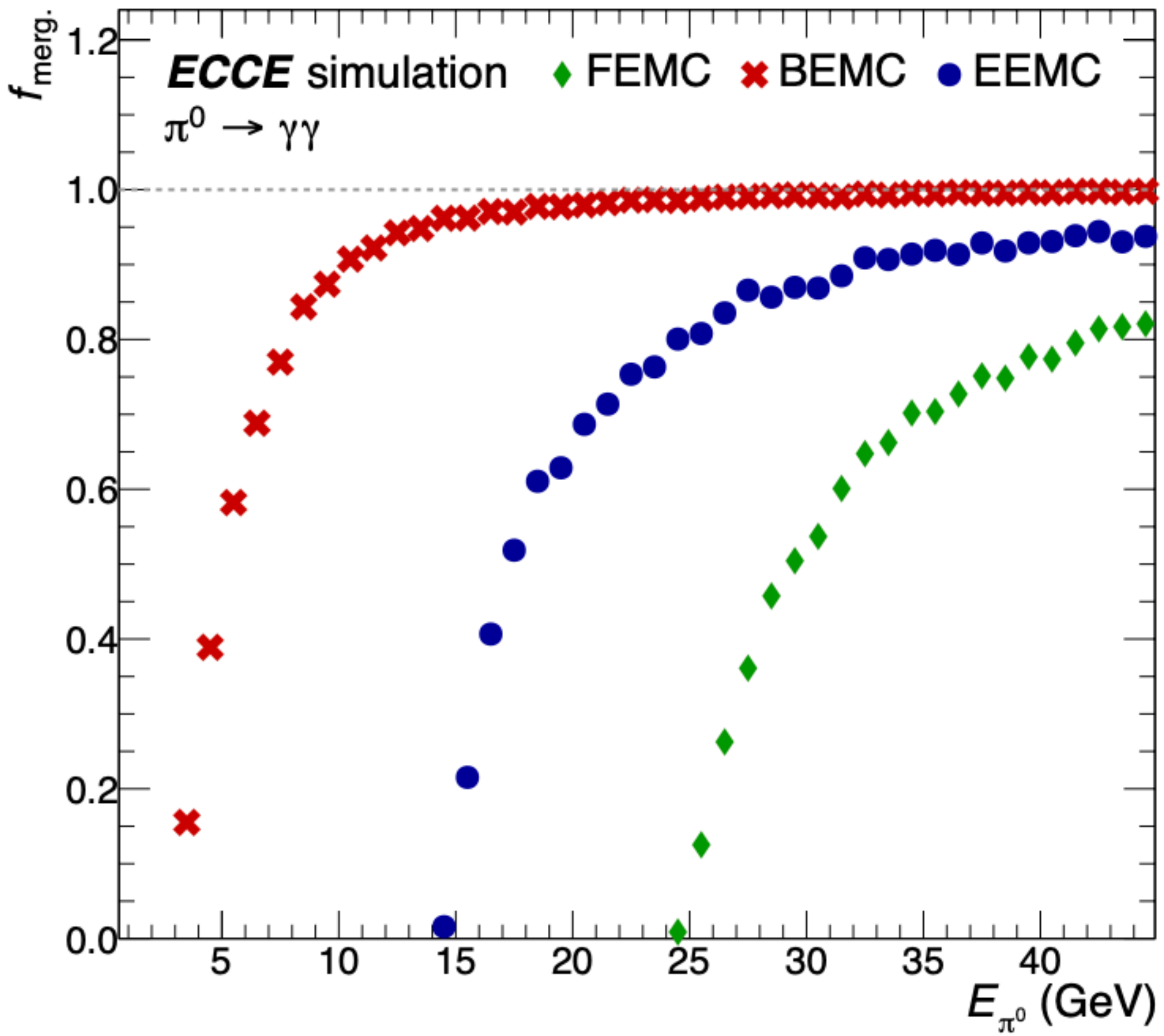

Figure 19: Fraction of neutral pions for which the showers from their decay photons are merged into a single cluster and can not be reconstructed using an invariant-mass-based approach for the different ECals.

Prompt searches:

- The signal is clean:

$$2\gamma + \text{recoiled } e^- + \text{intact lead ion}$$

- Basic cuts:
  - Due to the angular acceptance, we require $|\eta_\gamma| < 3.5$
  - To ensure an excellent photon resolution, we require $E_\gamma > 1 \text{ GeV}$
  - Perform a resonance search in the invariant mass of two photons

$$m_{\gamma\gamma} \in [m_a - \Delta m_{\gamma\gamma}/2, m_a + \Delta m_{\gamma\gamma}/2]$$

  - From a simulation:

$m_{\gamma\gamma}$ [GeV]	0.3	0.5	0.7	0.9	2.0	4.0	7.0	15.0
$\Delta m_{\gamma\gamma}/m_{\gamma\gamma}$ (%)	3.5	3.3	3.1	2.8	1.7	1.2	0.97	0.72

Backgrounds: light-by-light scattering

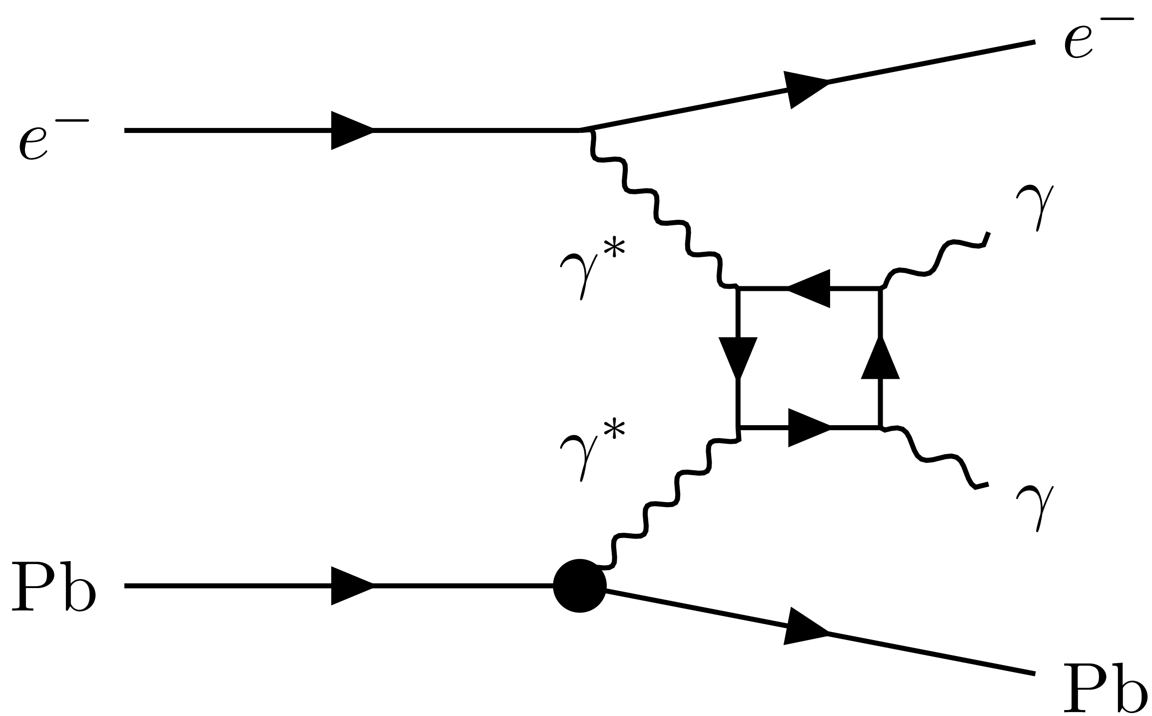

- **Irreducible** light-by-light (LBL) scattering: $\gamma + \gamma \to \gamma + \gamma$

$$\left.\frac{\sigma_{\rm sig}}{\sigma_{\rm LBL}}\right|_{\sqrt{\hat{s}}=m_a} \simeq \left(\frac{m_a}{1.0\,{\rm GeV}}\right)^3 \left(\frac{\rm TeV}{\Lambda}\right)^2 \left(\frac{200\,{\rm MeV}}{\Delta m_{\gamma\gamma}}\right)$$

Backgrounds: pion-pair production

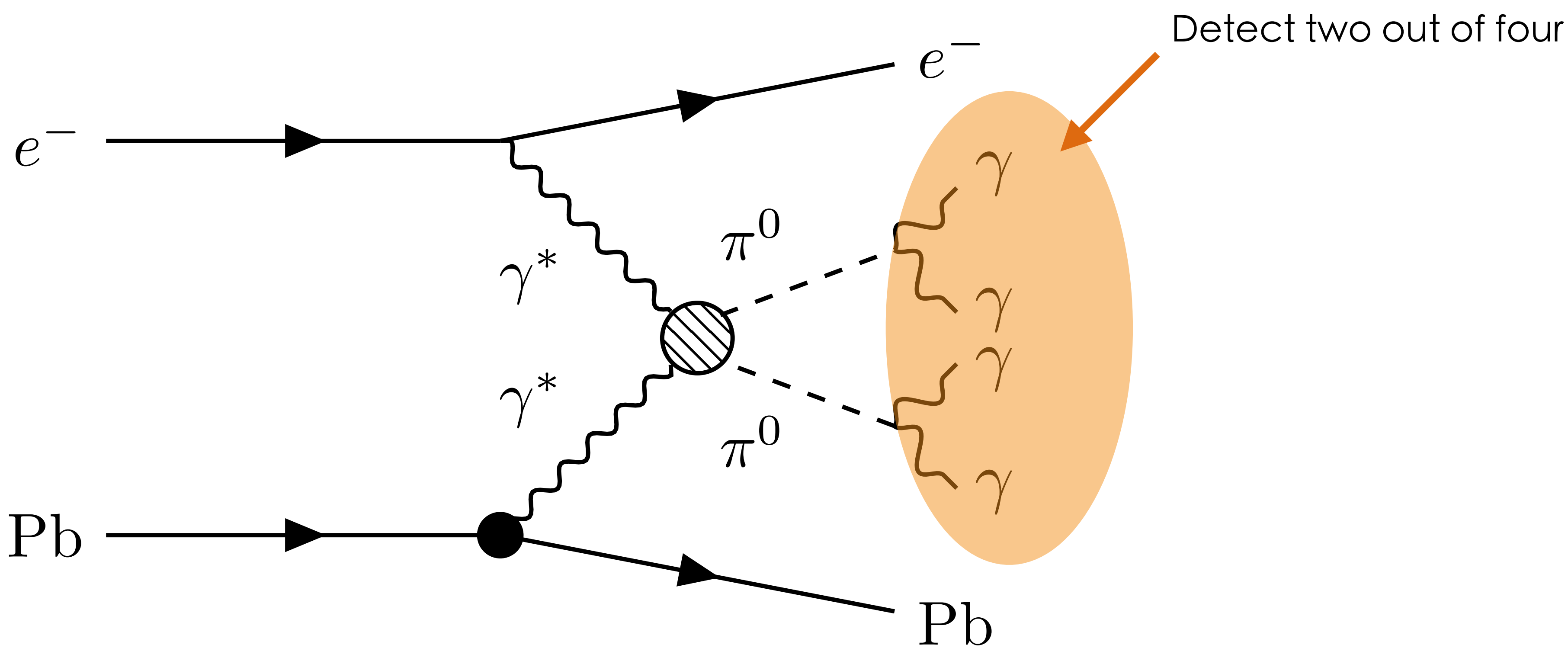

- **Reducible** Pion-pair production $\gamma + \gamma \to \pi^0 + \pi^0 \to 4\gamma$

Miss two photons: $p_N^{\mathrm{rec},2} = (p_N^{\mathrm{true}} + p_{\gamma_1}^{\mathrm{miss}} + p_{\gamma_2}^{\mathrm{miss}})^2 > m_N^2$

Require: $p_N^{\mathrm{rec},2} \leq (1.1\, m_N)^2 \qquad |\Delta\phi_{\gamma\gamma} - \pi| < 0.2$

Backgrounds: omega production

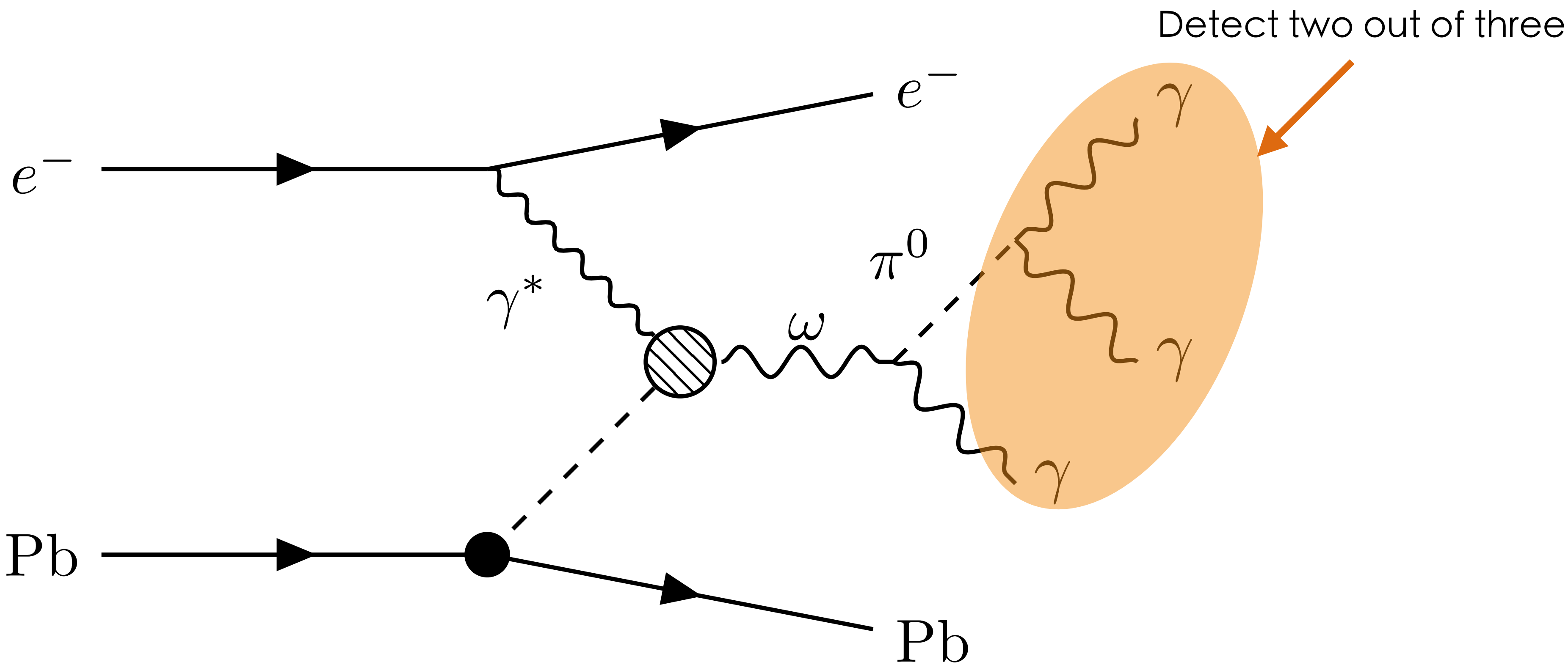

- **Reducible** $\omega\,(782) : \gamma + N \to \omega + N, \omega \to \pi^0 + \gamma \to 3\gamma$

Further require: $\eta_{\gamma_{1,2}} < 0$ if $m_{\gamma\gamma} < m_\omega$

EIC projections: prompt searches

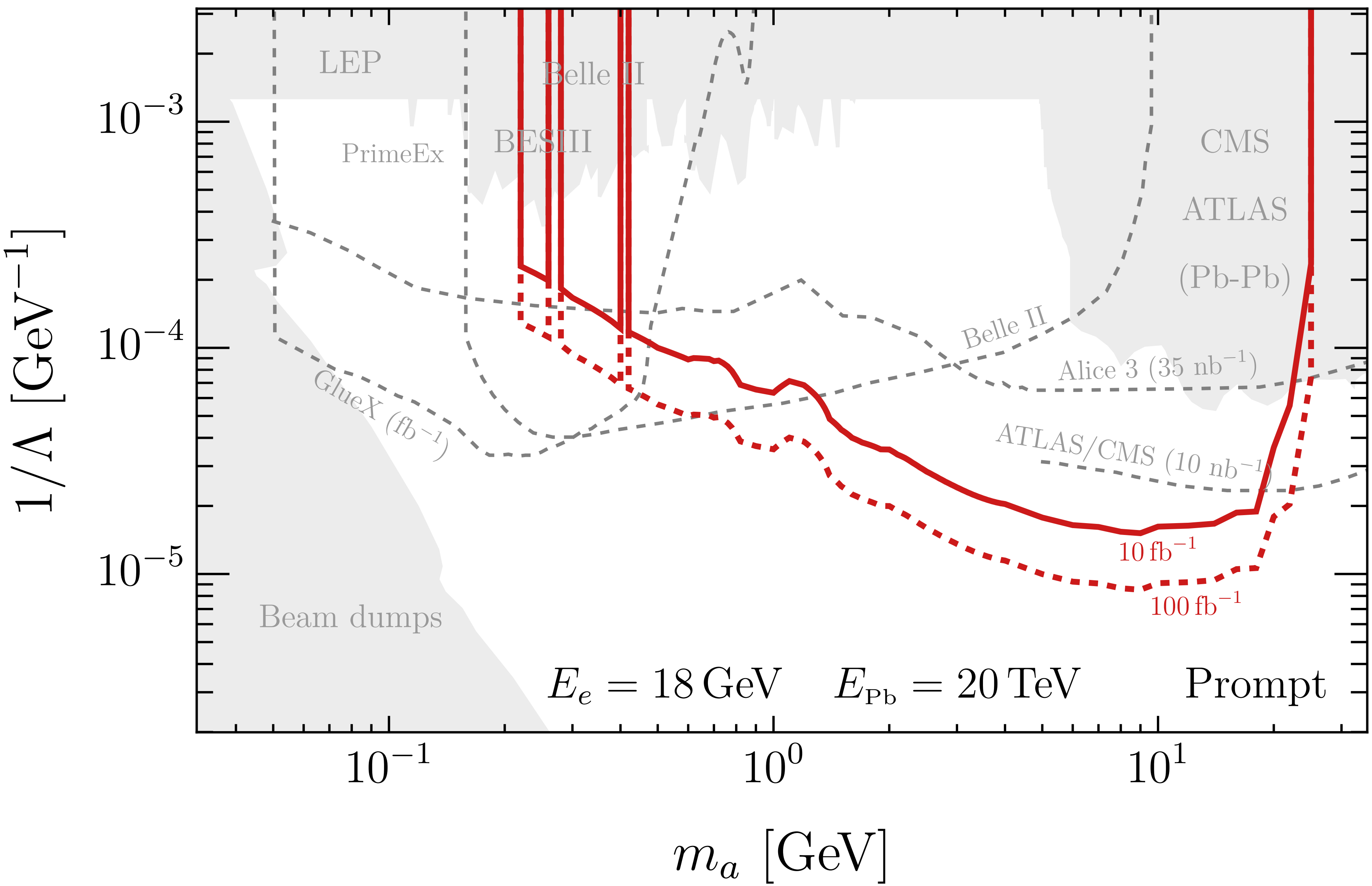

EIC projections: displaced-vertex searches

- Only basic cuts are applied
- $\mathcal{L} = 100\ \mathrm{fb}^{-1}$

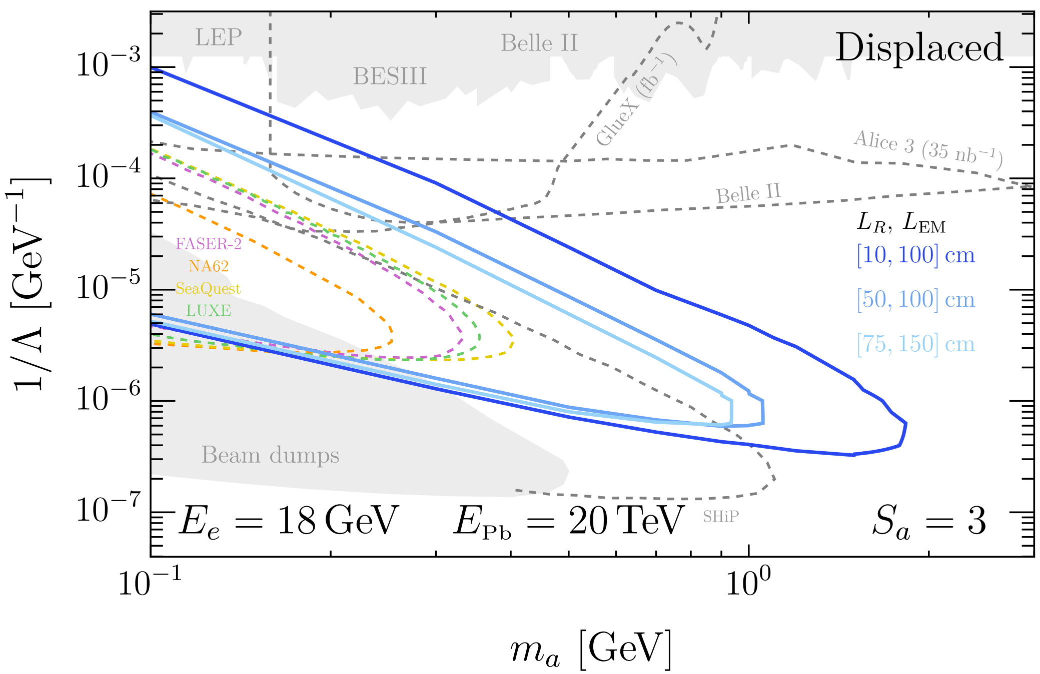

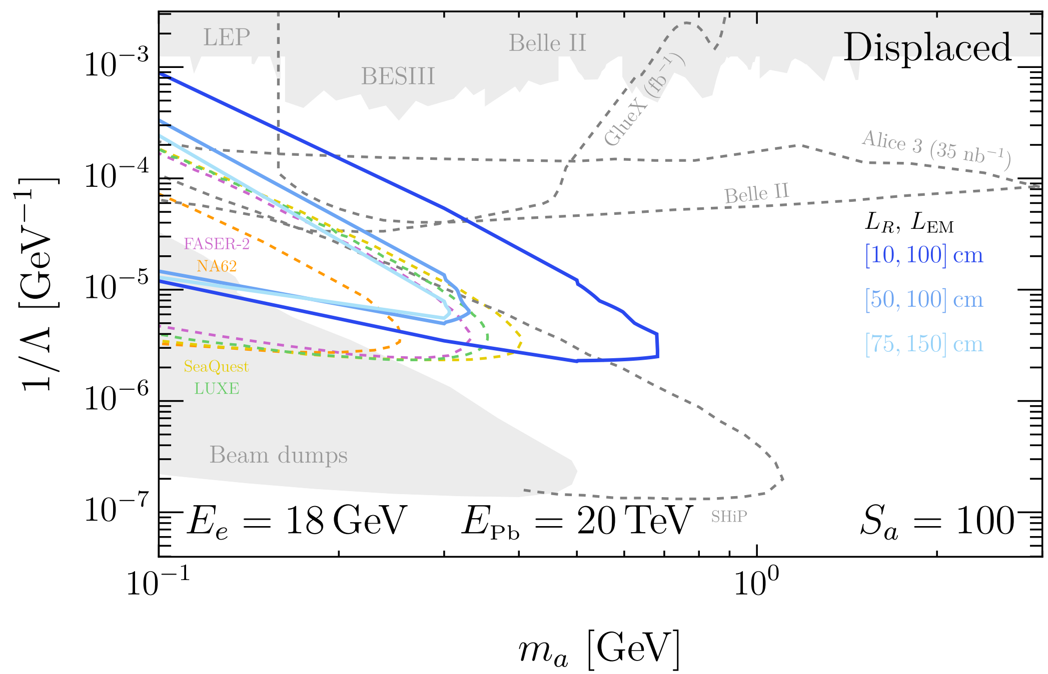

- Background free
- Bounds are set by $S_a = 3$

- Flat background $2500\ (\mathcal{L}/100\ \mathrm{fb}^{-1})$
- Bounds are set by $S_a/\sqrt{B} = 2$

Summary

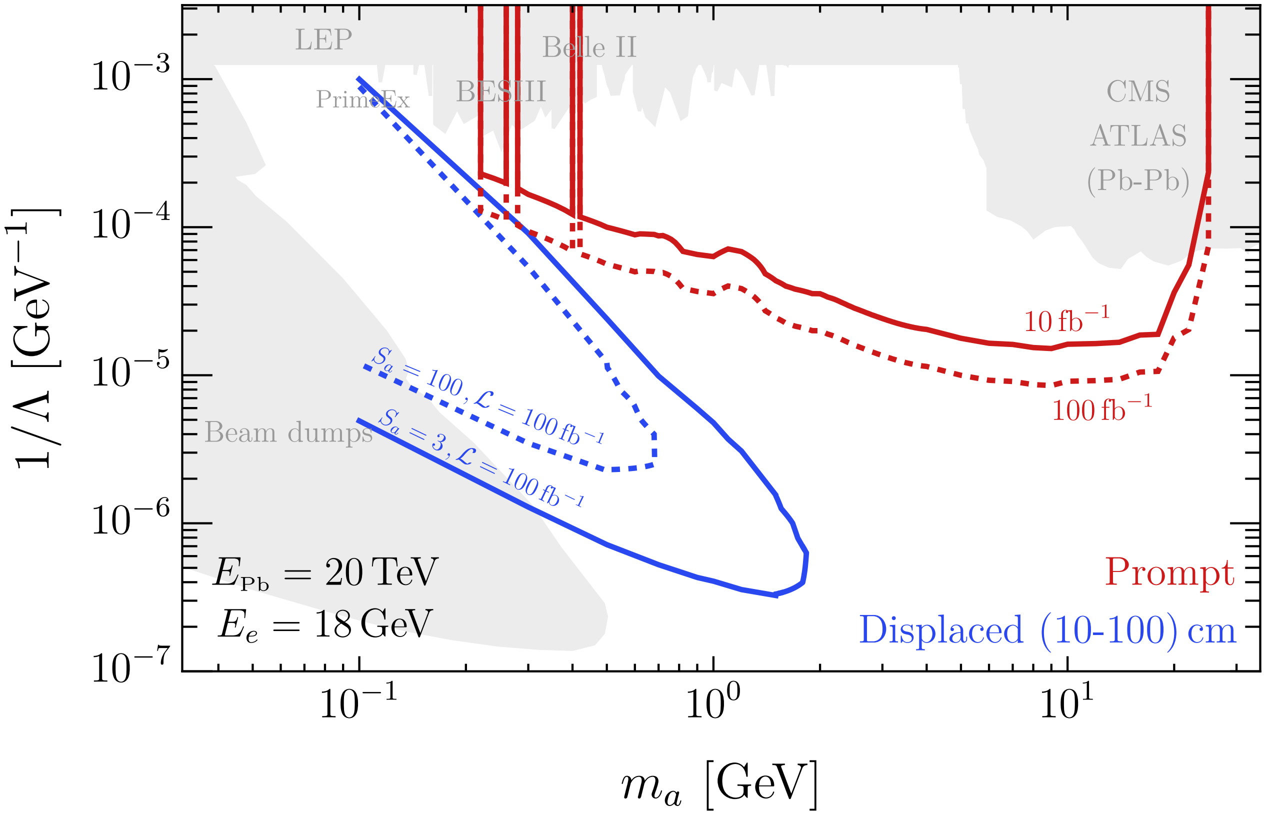

- EIC is good at detecting coherent process.

- EIC can surpass the current lepton and hadron collider and future heavy-ion projection due to the large ALPs production cross section and high luminosity.

- EIC can reach $\Lambda \sim 10^5$ GeV in the 2 to 20 GeV range in the prompt searches. For displaced-vertex search, it can reach $\Lambda \sim 10^7$ GeV for GeV ALPs.

Thanks!

Back-up slides

2-to-3 phase space

$$\Phi_3(s, m_e^2, m_N^2, m_a^2) = \int d^4p_e d^4p_N d^4p_a \delta(p_e^2 - m_e^2)\delta(p_N^2 - m_N^2)\delta(p_a^2 - m_a^2)$$
$$\times\delta^4(k_e + k_N - p_e - p_N - p_a)\theta(p_e^0)\theta(p_N^0)\theta(p_a^0)$$

There are five independent kinematical variables. However, the integration over the azimuthal angle is trivial.

$$t_e \equiv (k_e - p_e)^2 \qquad t_N \equiv (k_N - p_N)^2 \qquad m_{aN}^2 \equiv (p_a + p_N)^2 \qquad \cos\theta \equiv \frac{(\vec{k}_N \times \vec{p}_N)\cdot(\vec{k}_e \times \vec{p}_e)}{|\vec{k}_N \times \vec{p}_N||\vec{k}_e \times \vec{p}_e|}$$

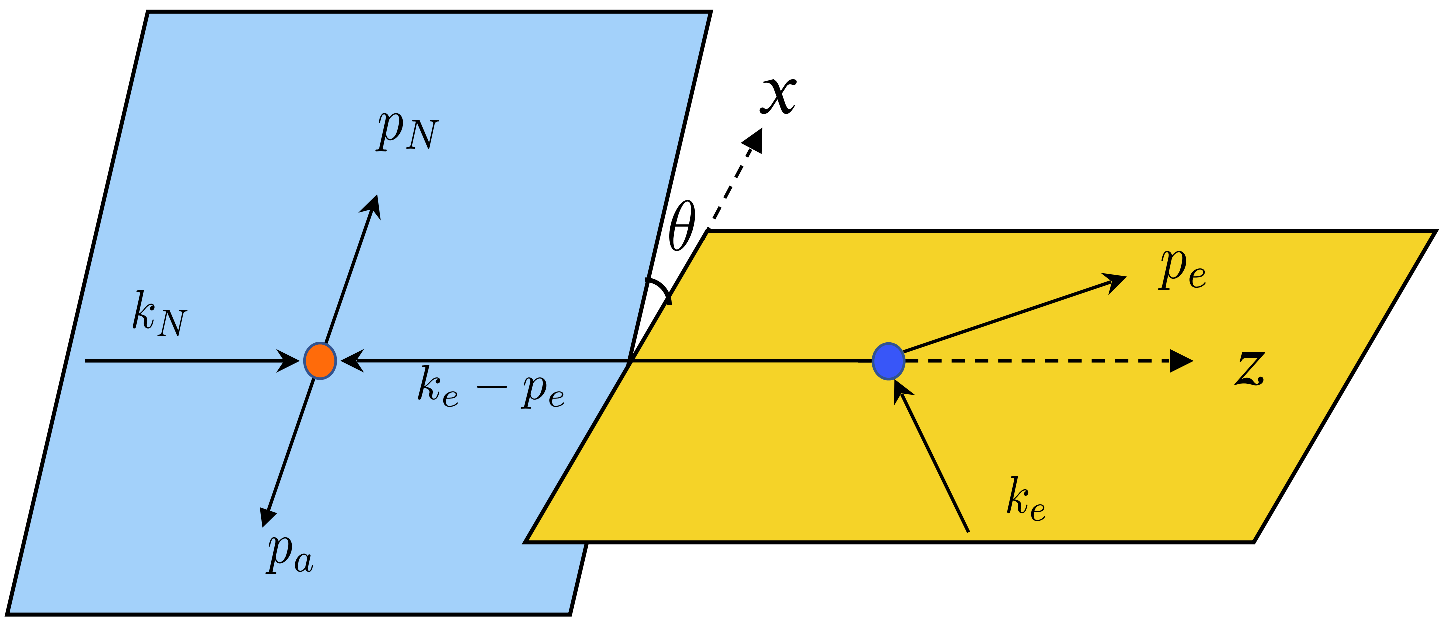

Cross sections after the cuts

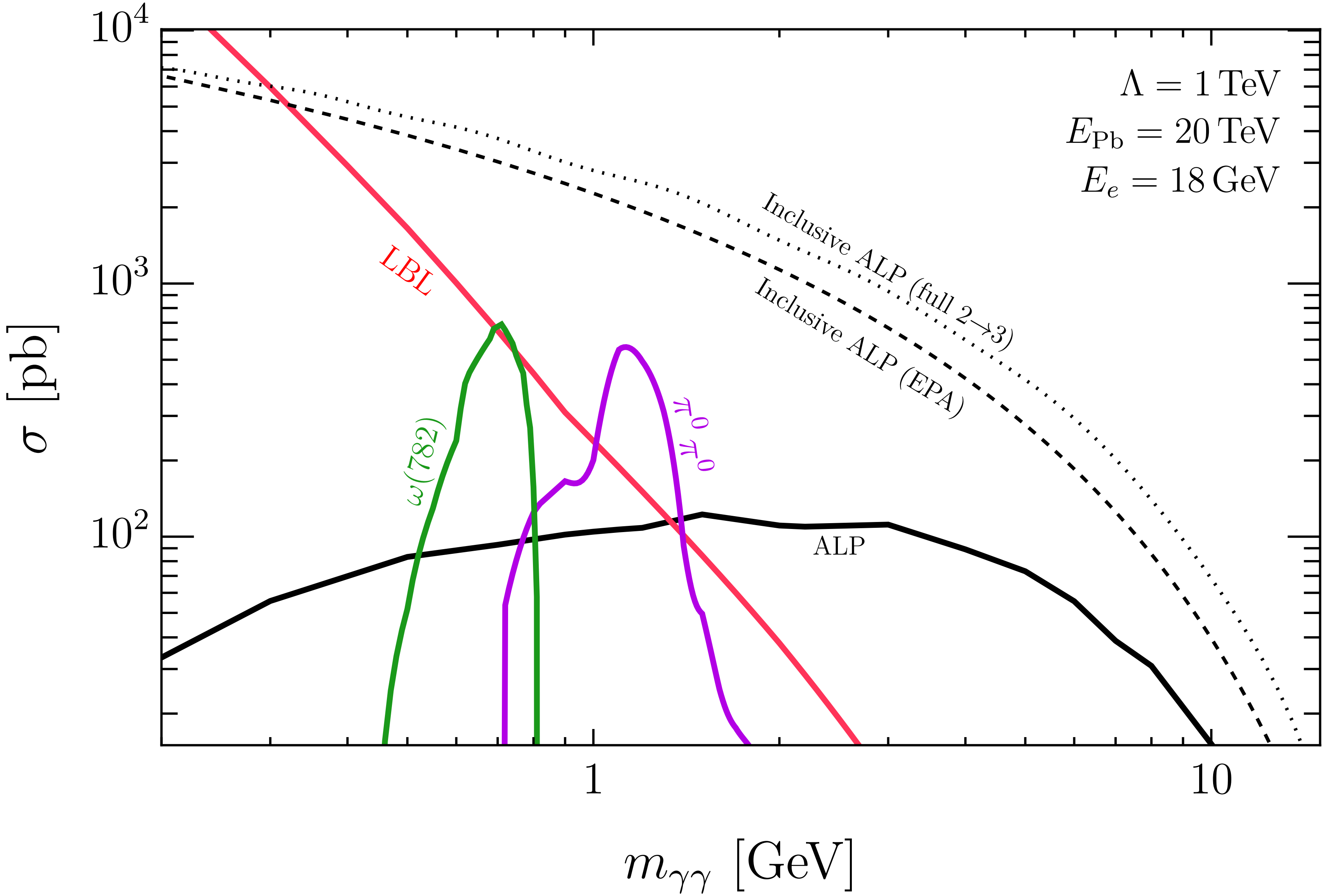

Electron ion collider

Calorimeter	Pseudorapidity acceptance	Projected energy resolution $(\Delta E/E)$ [%]
FEMC	$[+1.3\,,\,+3.5]$	$7.1/\sqrt{E/\mathrm{GeV}}$
BEMC	$[-1.7\,,\,+1.3]$	$1.6/\sqrt{E/\mathrm{GeV}} \oplus 0.7$
EEMC	$[-3.5\,,\,-1.7]$	$1.8/\sqrt{E/\mathrm{GeV}} \oplus 0.8$

FEMC: Hadron/Forward-End-Cap Electromagnetic Calorimeter
BEMC: Barrel Electromagnetic Calorimeter
EEMC: Electron-End-Cap Electromagnetic Calorimeter

	EEMC	BEMC	FEMC
tower size	2x2x20 cm^3	4x4x45.5 cm^3 projective projective	in: 1x1x37.5 cm^3 out: 1.6x1.6x37.5 cı out: 1.6x1.6x37.5 cı
material	$PbWO_4$	SciGlass	Pb/Scintillator
d_{abs}	-	-	1.6 mm
d_{act}	20 cm	45.5 cm	4 mm
N_{layers}	1	1	66
$N_{towers(channel)}$	2876	8960	19200/34416
X/X_O	~ 20	~ 16	~ 19
R_M	2.73 cm	3.58 cm	5.18 cm
f_{sampl}	0.914	0.970	0.220
λ/λ_0	~ 0.9	~ 1.6	~ 0.9
η acceptance	$-3.7 < \eta < -1.8$	$-1.7 < \eta < 1.3$	$1.3 < \eta < 4$
resolution			
- energy	$2/\sqrt{E} \oplus 1$	$2.5/\sqrt{E} \oplus 1.6$	$7.1/\sqrt{E} \oplus 0.3$
- φ	~ 0.03	~ 0.05	~ 0.04
- η	~ 0.015	~ 0.018	~ 0.02

[2209.02580]

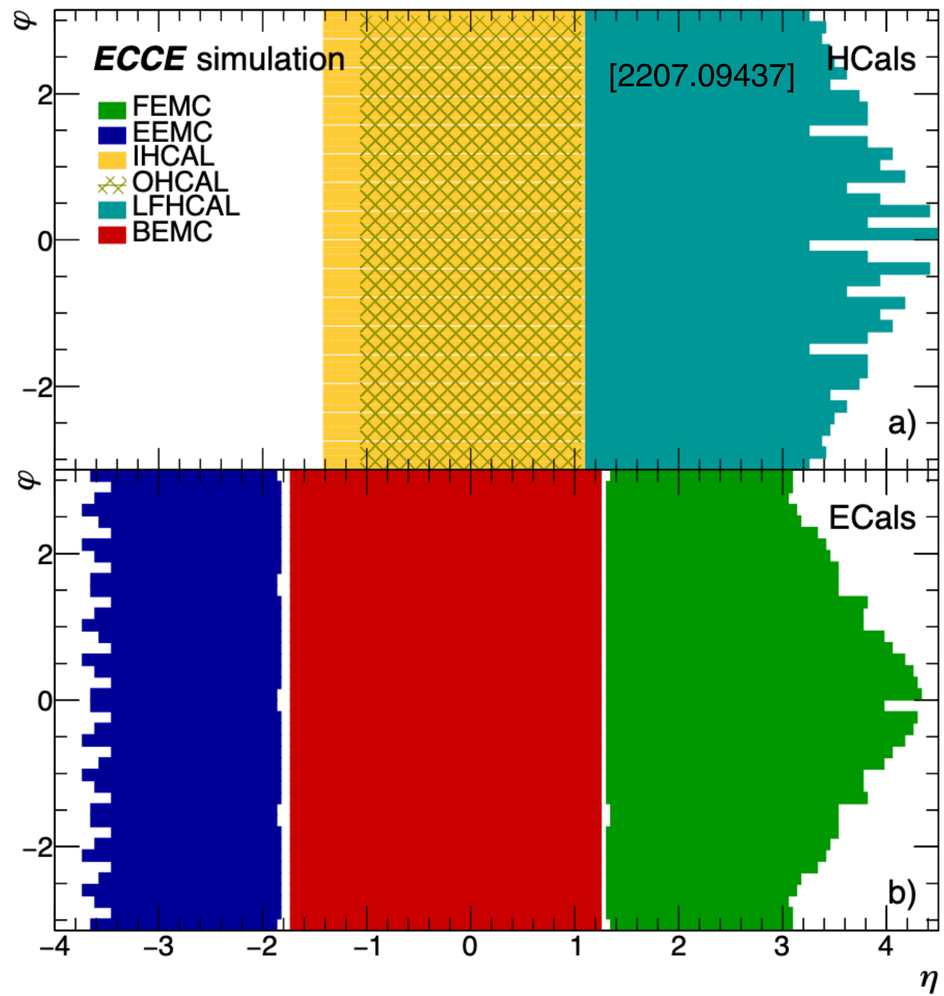

Kinematics

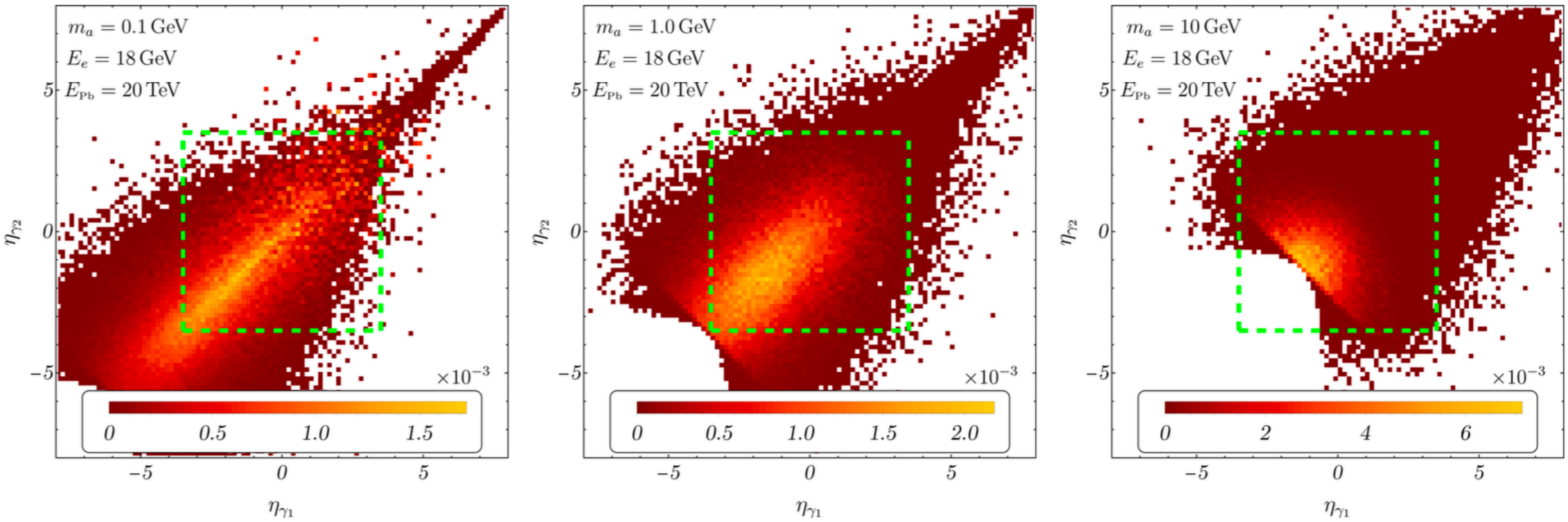

$m_a = 0.1\,\mathrm{GeV}$
$E_e = 18\,\mathrm{GeV}$
$E_{\mathrm{Pb}} = 20\,\mathrm{TeV}$
$\times 10^{-3}$
0 0.5 1.0 1.5
η_{γ_2}
η_{γ_1}
$m_a = 1.0\,\mathrm{GeV}$
$E_e = 18\,\mathrm{GeV}$
$E_{\mathrm{Pb}} = 20\,\mathrm{TeV}$
$\times 10^{-3}$
0 0.5 1.0 1.5 2.0
η_{γ_2}
η_{γ_1}
$m_a = 10\,\mathrm{GeV}$
$E_e = 18\,\mathrm{GeV}$
$E_{\mathrm{Pb}} = 20\,\mathrm{TeV}$
$\times 10^{-3}$
0 2 4 6
η_{γ_2}
η_{γ_1}